



Preparation of osteoinductive – Antimicrobial nanocomposite scaffolds based on poly (D,L-lactide-co-glycolide) modified with copper – Doped bioactive glass nanoparticles

Polymers and Polymer Composites
Volume 30: 1–12
© The Author(s) 2022
Article reuse guidelines:
sagepub.com/journals-permissions
DOI: 10.1177/09673911221098231
journals.sagepub.com/home/ppc


Cristian Covarrubias¹ , Julián Bejarano², Miguel Maureira¹, Cecilia Tapia³, Mario Díaz¹, Juan P Rodríguez⁴, Humberto Palza², Fernando Lund⁵, Alfredo Von Marttens⁶, Pablo Caviedes^{7,8} and Mehrdad Yazdani-Pedram⁹

Abstract

The aim of this study was to explore the preparation of porous nanocomposite scaffolds with simultaneous osteogenic – antibacterial properties by incorporating copper – doped bioactive glass nanoparticles into Poly (D,L-lactide-co-glycolide) lactide:glycolide. Bioactive glass nanoparticles were synthesized by using sol–gel technique from the $\text{SiO}_2 - \text{P}_2\text{O}_5 - \text{CaO} - \text{Na}_2\text{O} - \text{CuO}$ system. Poly (D,L-lactide-co-glycolide) lactide:glycolide nanocomposite scaffolds with different nanoparticle contents were prepared by combined lyophilization/salt leaching. The in vitro bioactivity of the scaffolds was assessed in simulated body fluid, and cell viability and osteogenic differentiation assays were performed with stem cells. Antibacterial activity of the materials was assessed against *Staphylococcus aureus*. Copper – doped bioactive glass nanoparticles particles with ~70 nm in size and relatively crystalline structure were synthesized. Porous nanocomposite scaffolds prepared with the copper – doped nanoparticles are cytocompatible, promoted the mineralization of bone-like apatite in simulated body fluid, and stimulated the osteogenic differentiation of stem cells as judged by an increased activity the enzyme alkaline phosphatase. The antibacterial activity exhibited by the nanocomposite scaffolds was not statistically superior to that of the neat polymer scaffold. Development of greater antibacterial activity in these nanocomposites would requires further research primarily related to the synthesis of more amorphous and soluble copper – doped bioactive glass nanoparticles.

Keywords

Polymer nanocomposite scaffolds, bioactive glass, copper nanoparticles, bone, antimicrobial composites

Received 4 June 2021; accepted 11 April 2022

Introduction

Efforts are continuously being made in the field of biomaterials and tissue engineering to find well-designed biomaterials for bone tissue regeneration.¹ Bioactive nanocomposite scaffolds prepared by incorporating bioactive ceramic nanoparticles into biodegradable polymeric matrices appear as interesting materials that combine the bioactivity of the inorganic nanoparticles

¹Laboratory of Nanobiomaterials, Research Institute of Dental Sciences, Faculty of Dentistry, Universidad de Chile, Santiago, Chile

²Departamento de Ingeniería Química, Biotecnología y Materiales, Facultad de Ciencias Físicas y Matemáticas, Universidad de Chile, Santiago, Chile

³Programa de Microbiología y Micología, ICBM, Facultad de Medicina, Universidad de Chile, Santiago, Chile

⁴Laboratory of Cell Biology, INTA, University of Chile, Santiago, Chile

⁵Departamento de Física y CIMAT, Facultad de Ciencias Físicas y Matemáticas, Universidad de Chile, Santiago, Chile

⁶Department of Prosthesis, Faculty of Dentistry, University of Chile, Santiago, Chile

⁷Program of Molecular & Clinical Pharmacology, ICBM, Faculty of Medicine, University of Chile

⁸Center for Biotechnology & Bioengineering (CeBiB), Department of Chemical Engineering, Biotechnology & Materials, Faculty of Physical & Mathematical Sciences, Univ. of Chile

⁹Departamento de Química Orgánica y Físicoquímica, Facultad de Ciencias Químicas y Farmacéuticas, Universidad de Chile, Santiago, Chile

Corresponding author:

Cristian Covarrubias, Facultad de Odontología, Universidad de Chile, Olivos 943, Independencia, Santiago 8380544, Chile.

Email: ccovarrubias@odontologia.uchile.cl



Creative Commons Non Commercial CC BY-NC: This article is distributed under the terms of the Creative Commons Attribution-NonCommercial 4.0 License (<https://creativecommons.org/licenses/by-nc/4.0/>) which permits non-commercial use, reproduction and distribution of the work without further permission provided the original work is attributed as specified on the SAGE and Open Access pages (<https://us.sagepub.com/en-us/nam/open-access-at-sage>).

with the supporting properties of the 3D polymeric matrix, which promote cellular attachment, and growth, and mineral deposition.² Recently, one of the most appealing approaches to design bone repair biomaterials is to combine in a single multifunctional biomaterial several abilities.³ Bone healing is also substantially hindered when infection occurs, mainly after an open fracture. Also, in bone reconstruction surgery, osteomyelitis caused by bacterial infection is a severe and ever-present complication.⁴ Another major cause of the infected bone defect is chronic bacterial infections, such as periodontitis.⁵

Consequently, the development of bioactive materials with antibacterial properties would represent a valuable solution in preventing bone-related infections. Copper is an element that exhibits antimicrobial activity against several microorganisms, including bacteria, fungi, and viruses.⁶ Besides, copper has antifouling property by decreasing the adherence of microorganisms and enhances proliferation of endothelial cells and angiogenesis in vivo.⁷ The incorporation of copper ions into the bioactive glass structure is being explored as a strategy to generate bifunctional biomaterials with osteogenic-antimicrobial properties. Wu et al.⁸ prepared microsized copper – containing mesoporous bioactive glass (MBG), which promoted the expression of osteogenic markers and inhibited the viability of *Escherichia coli*. Bari et al.⁹ synthesized Cu-doped MBG with a particle size in the 170–200 nm range. Although no cytocompatibility and cell differentiation assays were performed, the particles and their ionic dissolution extracts exhibited antibacterial effect against bacteria strains and the ability to inhibit and disperse the biofilm. Zheng et al.¹⁰ synthesized Cu-containing BG particles with sizes of approximately $\sim 0.45 \mu\text{m}$, which showed no significant cytotoxicity towards stem cells and fibroblasts. Other studies have shown that microsized BG modified with different copper and zinc contents can exhibit different textures, bioactivity in simulated body fluid (SBF) and cytocompatibility.¹¹ These particles enabled the preparation of multifunctional microcomposite scaffolds with enhanced biological activity when incorporated into a polymer matrix.¹² To our best knowledge, the synthesis of copper – doped BG with a nanometric particle size ($<100 \text{ nm}$) as well as the properties of nanocomposite scaffolds produced with these types of nanoparticles has not been until now reported. Nanocomposites offer more substantial surface area, high surface reactivity,

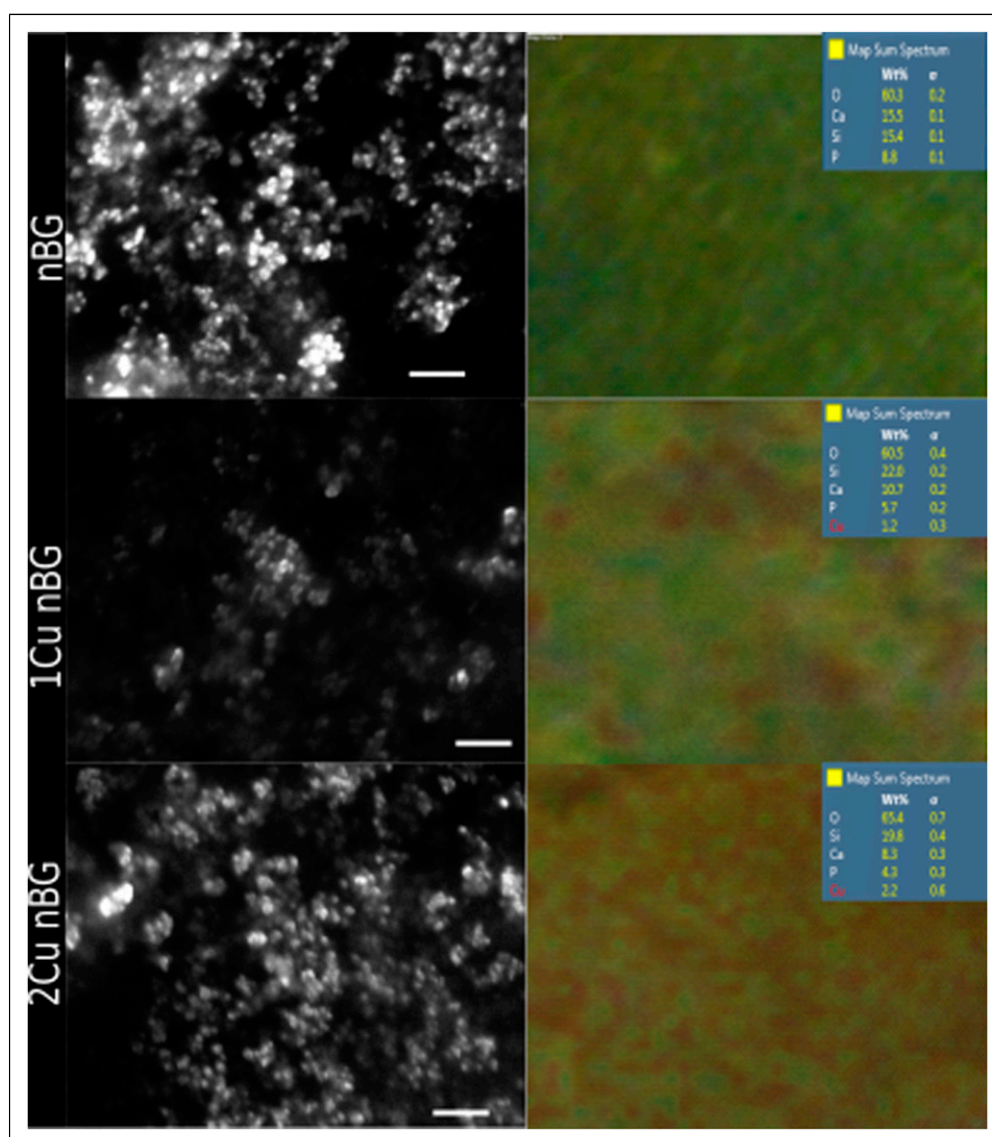


Figure 1. Scanning electron microscopy images and X-ray dispersive energy elemental mapping of nBG, 1Cu-nBG, and 2Cu-nBG nanoparticles.

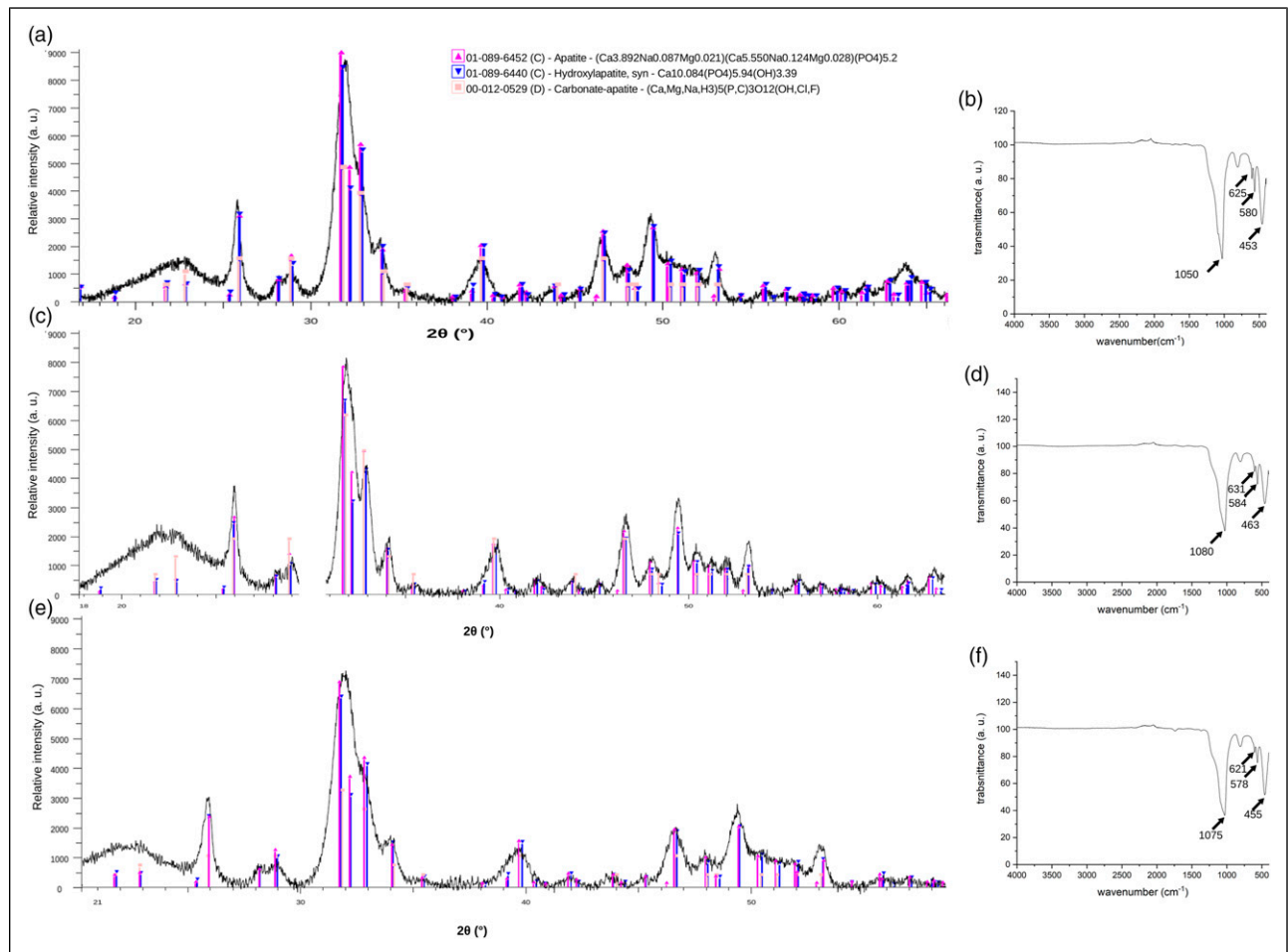


Figure 2. X-ray diffraction and total attenuated reflectance with Fourier transform infrared spectroscopy analyses of nBG, ICu-nBG, and 2Cu-nBG nanoparticles.

relatively strong interfacial bonding, design flexibility, and enhanced mechanical properties compared to conventional bulk composites.¹³ Our group systematically has studied the effect of nanoscale properties of BG with different nanostructure on its *in vitro* bioactivity and stem cell differentiation process.¹⁴ Nanocomposite scaffolds based on biodegradable polymers loaded with BG nanoparticles have shown the ability to promote the formation of bone-like apatite, stimulate stem cell differentiation into bone-forming osteoblast cells, and accelerate the bone tissue regeneration *in vivo*.^{15,16} Therefore, the challenge of the current work is to explore the preparation of bifunctional nanocomposite scaffolds exhibiting both osteoinductive and antibacterial properties by controlled incorporation of nanosized BG particles doped with copper into a PDLA polymer matrix.

Experimental

Materials

Poly (D,L-lactide-co-glycolide) lactide:glycolide (PDLA) (50:50), average molecular weight 406,000 g/mol, inherent viscosity 2.0 dL/g, and density 1.26 g/cm³ was purchased from Corbion-Purac Biochem (Gorinchem, Netherlands) and used without further processing. Tetraethylorthosilicate 98% (TEOS, Si(OC₂H₅)₄, CAS78-10-4), calcium nitrate tetrahydrate (Ca(NO₃)₂·4H₂O, CAS13477-34-4), ammonium phosphate monobasic (NH₄H₂PO₄, CAS7722-76-1), sodium nitrate (NaNO₃, CAS7631-99-4), 4-nitrophenyl phosphate disodium salt solution (pNPP, CAS 4264-83-9), and Bicinchoninic Acid Kit for Protein Determination (BCA) were purchased from Sigma-Aldrich (St. Louis, MO, USA). Copper nitrate trihydrate (Cu(NO₃)₂·3H₂O, CAS10031-43-3), ammonia solution 28–30% (NH₄OH, CAS1336-21-6), nitric acid (HNO₃, CAS7697-37-2), sodium chloride (NaCl, CAS7647-14-5), sodium hydroxide (NaOH, CAS1310-73-2), magnesium chloride (MgCl₂, CAS7786-30-3), and Tris (hydroxymethyl)aminomethane GR for analysis buffer (TRIS-buffer, CAS77-86-1) were purchased from Merck (Darmstadt, Germany). Dulbecco's modified Eagle medium (Alpha-MEM) was purchased from Invitrogen Life Technologies (Carlsbad, CA, USA). 10% Gibco™ fetal bovine serum (FBS), 100 U penicillin, and 100 mg/mL streptomycin were purchased from Thermo Fisher Scientific (Asheville, USA). 3-(4,5-dimethyl-thiazol-2-yl)-5-(3-carboxymethoxyphenyl)-2-(4-sulfophenyl)-2H-tetrazolium] (MTS) and an electron coupling reagent (phenazine ethosulfate; PES) (CellTiter Aqueous One Solution cell proliferation assay kit) was purchased from Promega (Madison, WI, USA). Brain Heart Infusion (BHI) with 6.5% sodium chloride and BHI Agar were purchased from Becton Dickinson (Mountainview, CA, USA). Polysorbate 80 surfactant was purchased from Difco Laboratories (Tween® 80, Detroit, MI, USA).

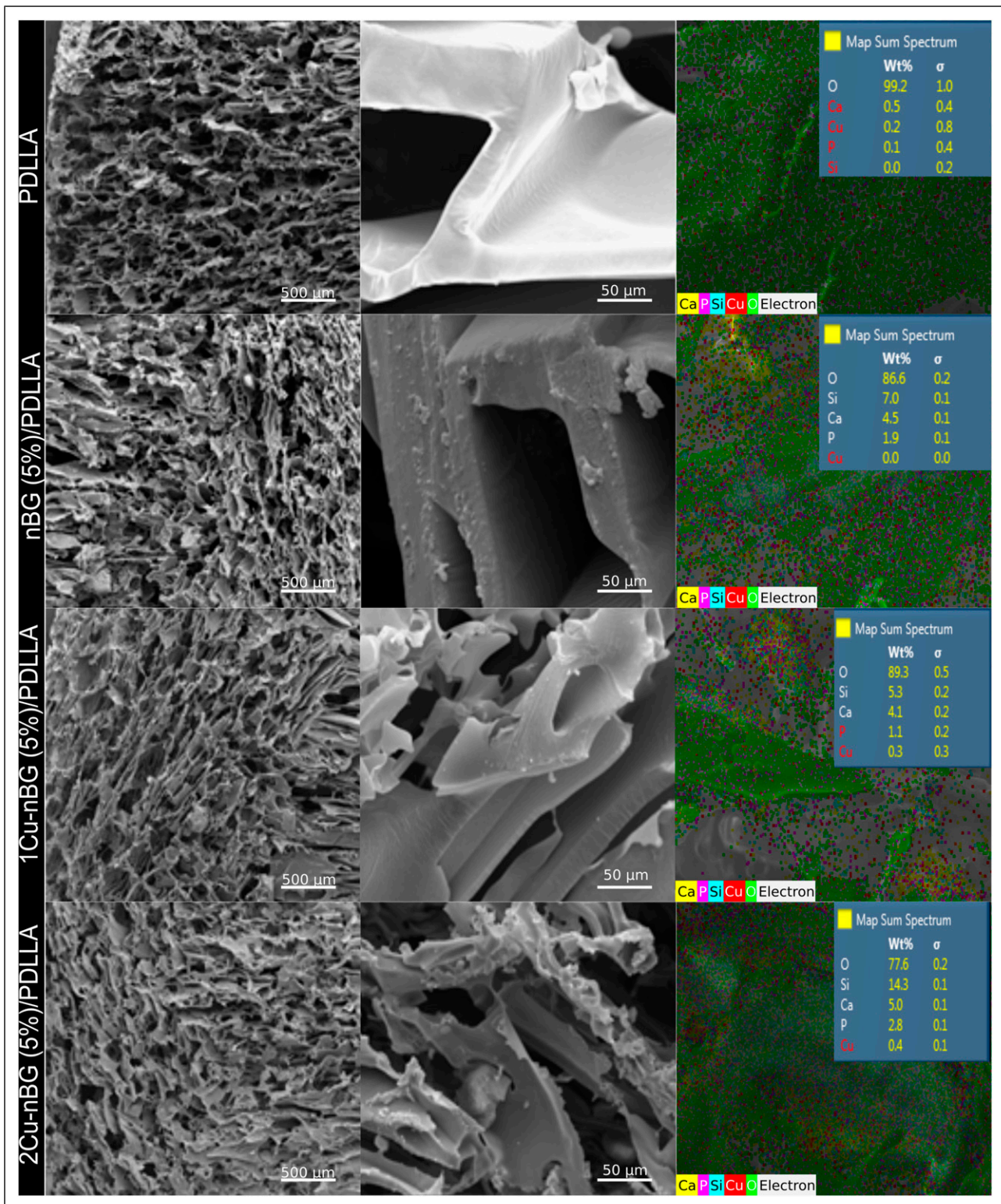


Figure 3. Scanning electron microscopy images and X-ray dispersive energy elemental mapping of PDLLA, nBG (5%)/PDLLA, 1Cu-nBG (5%)/PDLLA, and 2Cu-nBG (5%)/PDLLA nanocomposite scaffolds. PDLLA: Poly (D,L-lactide-co-glycolide).

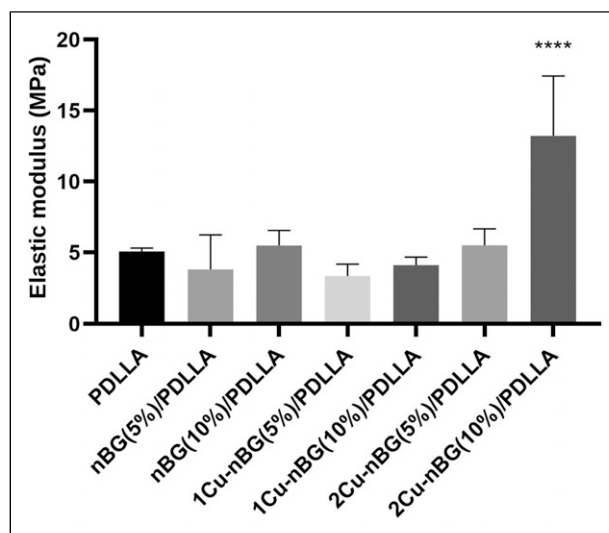
Synthesis of nanoparticles

nBG nanoparticles with a molar composition of $60\text{SiO}_2 : 25\text{CaO} : 11\text{Na}_2\text{O} : 4\text{P}_2\text{O}_5$ (mol %) were prepared by the sol-gel method as out as follows: a calcium-based solution was prepared by dissolving $\text{Ca}(\text{NO}_3)_2 \times 4\text{H}_2\text{O}$ and NaNO_3 in distilled water at room temperature. A second solution was prepared by diluting TEOS in ethanol, and it was added to the calcium nitrate solution, and the pH of the resulting solution was adjusted to 1–2 with nitric acid. This transparent solution was slowly dropped under vigorous stirring into a solution of $\text{NH}_4\text{H}_2\text{PO}_4$ in 1500 mL of distilled water. During the dripping process the pH was kept at around 10 with aqueous ammonia. The mixture was stirred for 48 h and aged for 48 h at room temperature. The

Table 1. Porosity measurements of neat poly (D,L-lactide-co-glycolide) and nanocomposite scaffolds.

Scaffold	Porosity (%)	SD
PDLLA	91.9	1.0
nBG (5%)/PDLLA	90.7	0.7
nBG (10%)/PDLLA	89.9	1.2
1Cu-nBG (5%)/PDLLA	88.9	1.5
1Cu-nBG (10%)/PDLLA	89.8	1.2
2Cu-nBG (5%)/PDLLA	92.0	1.2
2Cu-nBG (10%)/PDLLA	90.2	2.4

PDLLA: Poly (D,L-lactide-co-glycolide).

**Figure 4.** Compressive elastic modulus of neat poly (D,L-lactide-co-glycolide) and nanocomposite scaffolds.

precipitate was separated by centrifugation (12,000 rpm) and washed by three centrifugation-redispersion cycles with distilled water. This suspension was freeze dried and then calcined at 700°C for 3 h to obtain a fine white nBG powder. To prepare Cu-nBG nanoparticles 1 or 2 mol of calcium was replaced in first solution by $\text{Cu}(\text{NO}_3)_2$.

Preparation of nanocomposite scaffolds

The PDLLA nanocomposite scaffolds were fabricated using solvent casting-particulate leaching and freeze dryer processes from mixtures of PDLLA and nanometric bioactive glass. Briefly, PDLLA was dissolved in DMC solvent under magnetic stirring at room temperature for 2 h, using a polymer solvent at a ratio of 8% (w/v). Then, the nanoparticle powders (5 or 10 wt.%) were added to the polymer solution, and the resulting mixture was stirred for 30 min and sonicated for 15 min to ensure a homogeneous distribution of the glass particles in the polymer solution.

Then, NaCl particles sieved between 100 and 400 μm was added to the suspension in a ratio of 9:1 and stirred for 30 min. This mixture was then transferred to a Teflon dish and maintained at -80°C for 3 h before freeze dryer for 24 h. After that, the scaffolds left immersed in sterilized double-distilled water for 48 h, replacing it every 4 h to dissolve the salt completely and to leave a porous structure. Finally, porous discs of 150 mm in diameter and 4.5 mm in thickness were obtained, and these were dried at 30°C with vacuum for 48 h. For characterization, the scaffolds were cut using double-edged foil razor blades.

Material characterization

The materials and apatite formation in SBF were analysed by scanning electron microscopy (SEM) in an JEOL JSM-IT300LV microscope equipped with X-ray dispersive energy elemental microanalysis (EDX). Average particle size of nanoparticles was calculated from the arithmetic mean of 20 measurements using the software of the JEOL JSM-IT300LV microscope. Nanoparticle X-ray diffraction (XRD) analysis was carried in a Siemens D5000 X-ray powder diffractometer using $\text{CuK}\alpha$ radiation. The chemical structure of the materials was characterized by total attenuated reflectance with Fourier transform infrared spectroscopy (ATR-FTIR) using an Agilent Cary 630 ATR-FTIR spectrometer. Mechanical compression tests of $4 \times 4 \times 5$ mm scaffolds were performed with DEBEN microtest machine (Suffolk, UK) using a 2 N load cell in compression mode. Elastic modulus was obtained as the mean value of measuring four specimens.

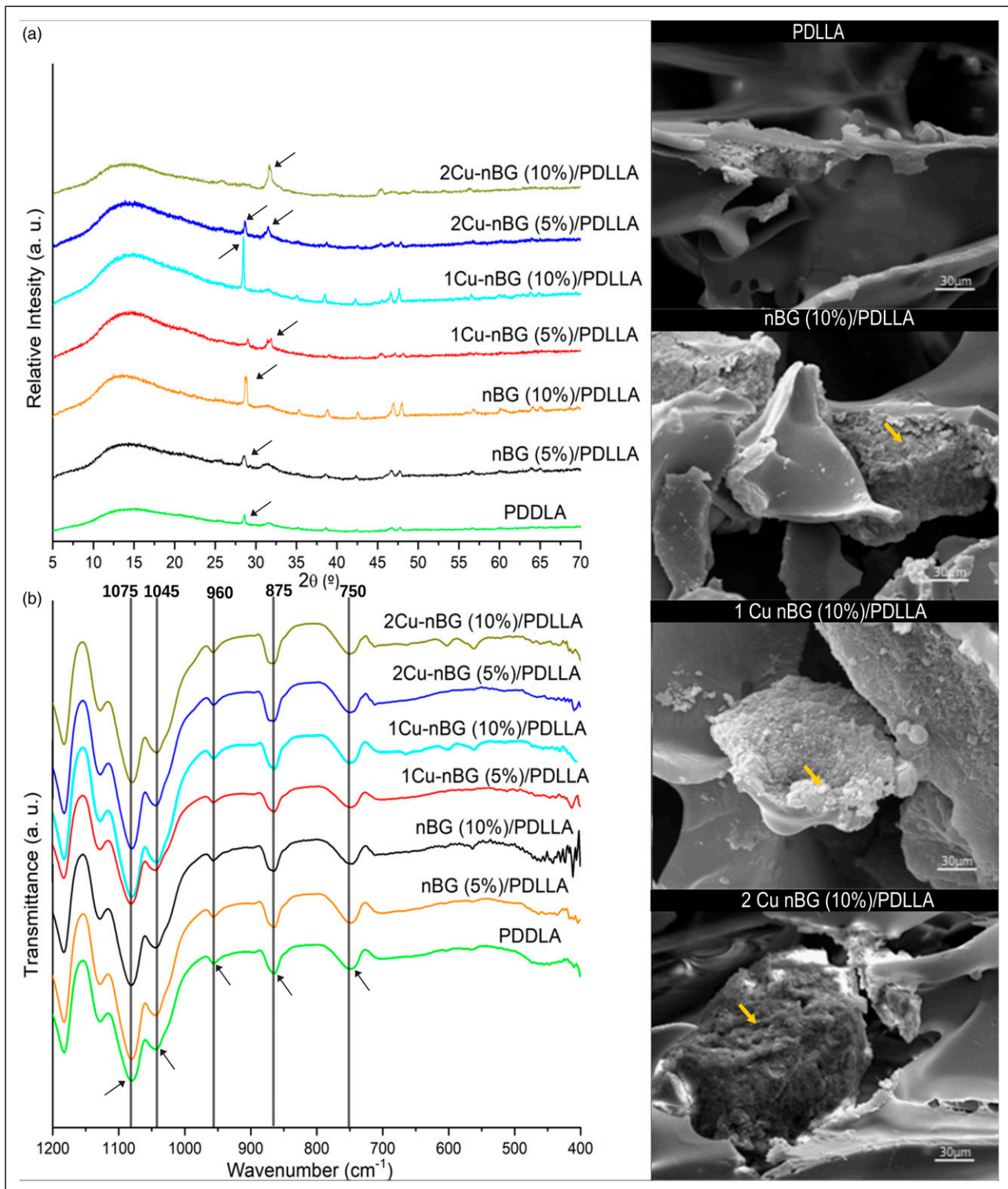


Figure 5. X-ray diffraction patterns, total attenuated reflectance with Fourier transform infrared spectroscopy spectra, and SEM images of PDLLA, nBG (5%)/PDLLA, nBG (10%)/PDLLA, 1Cu-nBG (5%)/PDLLA, 1Cu-nBG (10%)/PDLLA, 2Cu-nBG (5%)/PDLLA, and 2Cu-nBG (10%)/PDLLA nanocomposite scaffolds after conditioning in simulated body fluid for 7 days. PDLLA: Poly (D,L-lactide-co-glycolide).

The porosity of the scaffolds was estimated using the method of displaced volume. The densities of PDLLA non-porous films (ρ_{mat}) and of absolute ethanol (ρ_e) were measured with a pycnometer. A small piece of scaffold was weighed (W_s) and its volume calculated using $V_s = W_s/\rho_{\text{mat}}$. Then, scaffold was immersed for 20 min in absolute ethanol. The excess liquid was removed from the scaffold and the wet weight (W_f) was obtained. The weight (W_e) and volume (V_e) occupied by the ethanol inside the scaffold's porous network were calculated from the formula: $W_e = W_f - W_s$ and $V_e = W_e/\rho_e$, respectively. The porosity percentage of each scaffold was calculated as follows: Porosity (%) = $(V_e/(V_e + V_s)) \times 100$.

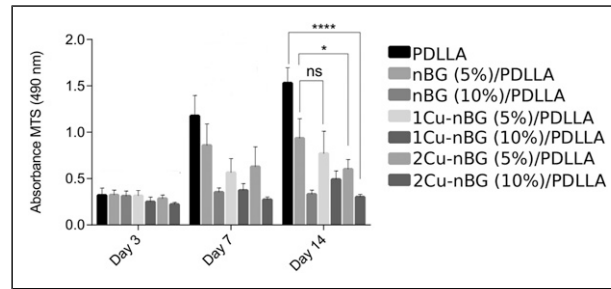


Figure 6. MTS viability of dental pulp stem cells cultured with PDLLA, nBG (5%)/PDLLA, nBG (10%)/PDLLA, 1Cu-nBG (5%)/PDLLA, 1Cu-nBG (10%)/PDLLA, 2Cu-nBG (5%)/PDLLA, and 2Cu-nBG (10%)/PDLLA nanocomposite scaffolds. PDLLA: Poly (D,L-lactide-co-glycolide).

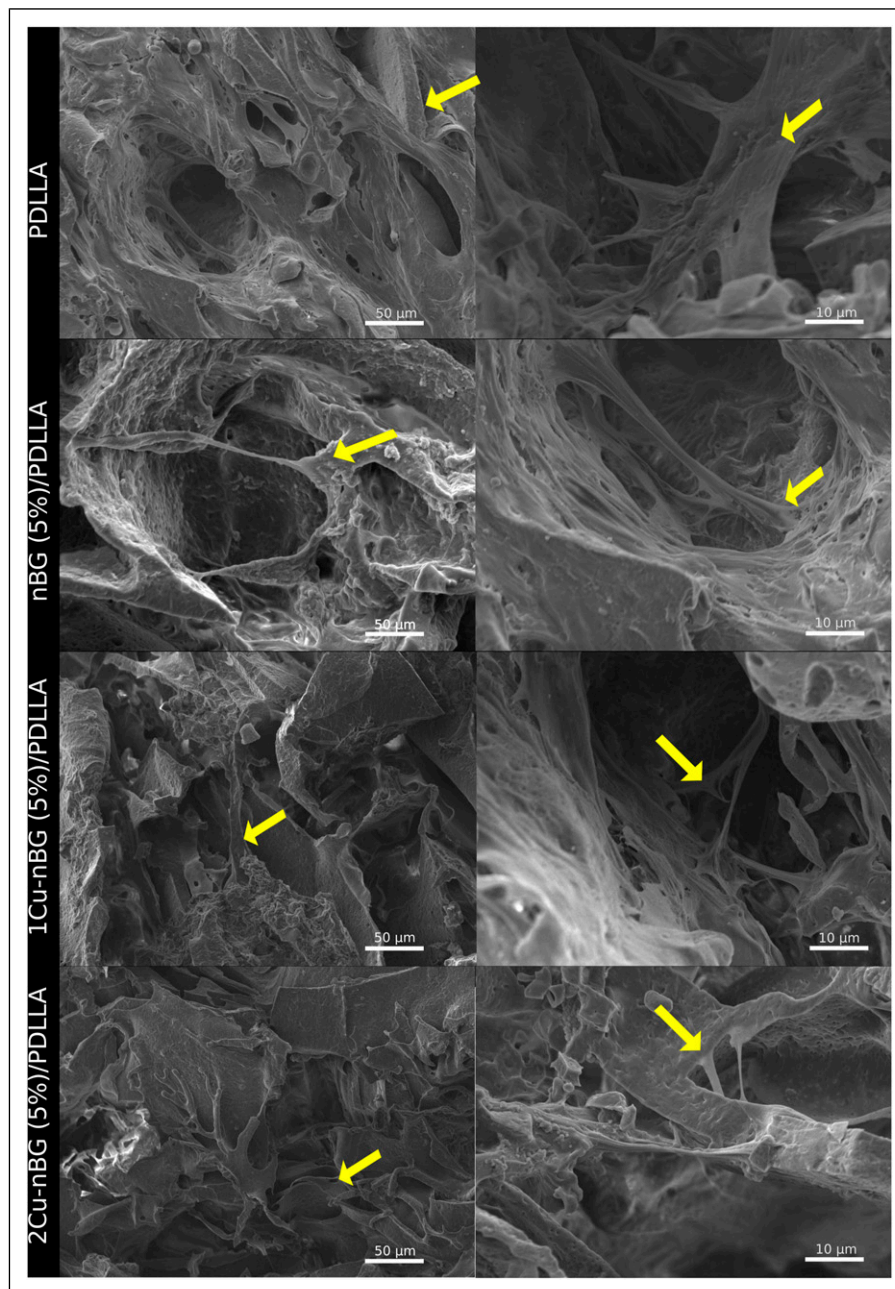


Figure 7. Scanning electron microscopy images of dental pulp stem cells adhered on the surface of neat PDLLA and on that of nanocomposite scaffolds loaded with 5% of nanoparticles after 7 days of incubation.

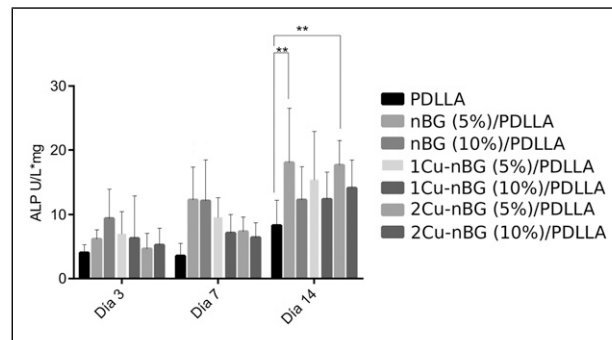


Figure 8. Alkaline phosphatase activity of dental pulp stem cells cultured with PDLLA, nBG (5%)/PDLLA, nBG (10%)/PDLLA, 1Cu-nBG (5%)/PDLLA, 1Cu-nBG (10%)/PDLLA, 2Cu-nBG (5%)/PDLLA, and 2Cu-nBG (10%)/PDLLA nanocomposite scaffolds in the absence of osteogenic supplements. PDLLA: Poly (D,L-lactide-co-glycolide).

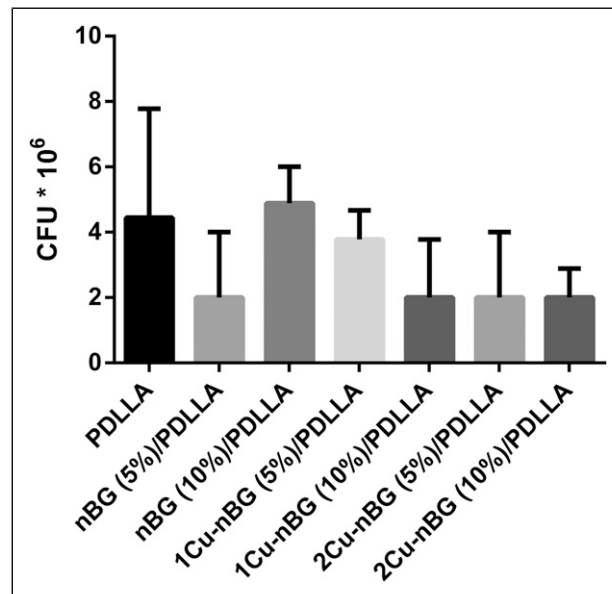


Figure 9. Antibacterial activity of the scaffolds expressed as the capacity of the material to inhibit the growth of viable colonies of *Staphylococcus aureus* on its surface.

In vitro bioactivity assays

The ability of the nanocomposites to induce the formation of apatite was assessed in acellular SBF, which has inorganic ion concentrations like those of human extracellular fluid. The SBF solution was prepared as described by Kokubo et al.¹⁷ using the standard ion composition and pH 7.4. The cylindrical nanocomposite samples (1.0 cm × 0.5 cm) were individually soaked in 50 mL of SBF in polyethylene containers at 36.5°C using a thermostatic bath. After incubation for 7 days, the scaffolds were removed from SBF, rinsed with distilled water, and dried at 60°C.

Cell culture

Stem cells isolated from human dental pulp (DPSCs) were used to evaluate cell proliferation and differentiation at 3, 7, and 14 days of incubation with the scaffold materials. DPSCs were cultured with the scaffolds in Alpha-MEM containing 10% FBS, 100U/mL penicillin, and 100 µg/mL streptomycin in absence of osteogenic supplements. Cell viability was measured using the MTS colorimetric assay (CellTiter 96[®] Aqueous MTS Reagent, Promega) at 490 nm. The enzymatic activity of alkaline phosphatase (ALP) was measured using the colorimetric ALP reaction buffer (Tris (0.1 M), MgCl₂ (2 mM), p-nitrophenol phosphate (9 mM), pH 9.8) at 405 nm. The morphology of cells adhered on the scaffold surface after 7 days of incubation was examined by SEM microscopy. Adherent cells were fixed in a 2.5% glutaraldehyde solution, washed with PBS, dehydrated gradually by ethanol series, dried in a supercritical CO₂ drying (Autosamdri-815) and gold – coated using a Denton Vacuum sputter coater (Desk V) before being examined in the SEM microscope.

Antibacterial activity

The nanocomposite scaffolds were incubated in a 0.5 McFarland *Staphylococcus aureus* suspension in BHI with 6.5% sodium chloride for 24 h. Afterward, the surfaces were washed with a 0.88 wt% NaCl solution and 1% Tween 80 to remove the

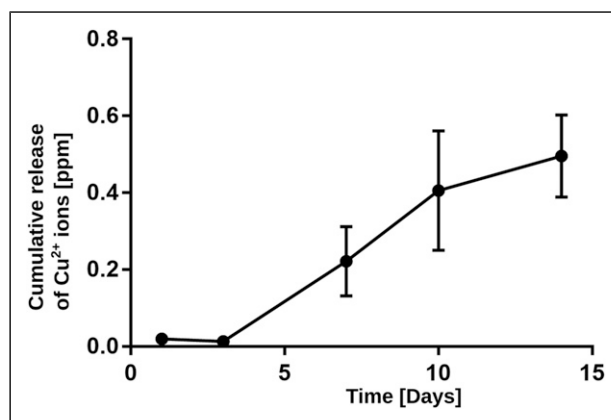


Figure 10. Cumulative Cu²⁺ release from 1Cu-nBG (10%)/poly (D,L-lactide-co-glycolide) nanocomposite scaffold immersed in phosphate buffered saline.

bacteria grown on the surface. Samples of 100 μ L were taken from the bacterial suspension, diluted, and plated in BHI agar. After 48 h of incubation at 37°C, the colonies were counted and the colony forming units per mL were calculated.¹⁸

Statistical analysis

Cell results were expressed as mean \pm SD, with $n = 9$ per group and time point for, MTS, and ALP assays and $n = 3$ for antibacterial activity. Data were analysed employing one-way analysis with post hoc multiple comparisons achieved using Tukey's test by using GraphPad prism 6 (GraphPad Software, San Diego, CA, USA). Differences were significant when $p < .05$.

Copper release measurements

The release of Cu ions from a representative nanocomposite scaffold was measured in phosphate buffered saline (PBS) (pH 7.4) at 37°C. $2 \times 2 \times 2$ cm scaffold piece was immersed in 20 mL of PBS up to 14 days of incubation. The Cu ion concentration in the aqueous phase was analyzed at different time intervals with a Cupric Sulfide/Silver Sulfide Solid – State Combination Ion Selective Electrode (Hanna HI4108).

Results and discussion

Figures 1 and 2 show the structural characterization of the nBG particles and those synthesized in the presence of copper ions. Average particle size of 1Cu-nBG and 2Cu-nBG was of ~ 70 nm as estimated from SEM measurements, and their EDX copper contents were of 1.2 and 2.2 wt. %, respectively (Figure 1). XRD patterns of the nanoparticles exhibit reflections associated with structural ordering in the glass. Although nBG with an amorphous structure is typically obtained from the sol-gel synthesis composition SiO₂–CaO–P₂O₅,¹⁵ bioactive glasses with crystalline structures have been observed when the quaternary system 60SiO₂: 25CaO:11Na₂O: 4P₂O₅ is used.^{19,20} Identification of the XRD reflections revealed the presence apatite – related crystalline phases in the nanoparticles (Figure 2), which are also responsible of the FTIR vibrations at 590, 601 and 1100 cm⁻¹ corresponding to the P – O deformations modes of phosphate in apatite.²¹ The results also indicate that no changes in the crystal structure of nBG occur after copper incorporation.

Figure 3 shows the SEM-EDX and ATR-FTIR analysis of the neat PDLLA scaffold and nanocomposites prepared with the 5 wt. % nanoparticle content. From SEM images, it can be observed that the scaffolds are composed by elongated pores with relatively uniform diameters in the 50–120 μ m range. Although microsized agglomerations of the nanoparticles can be detected on the polymer walls, EDX mapping of Si, P and Cu suggests a relatively uniform distribution of the nanoparticles into the polymer matrix. The nanocomposite scaffolds also exhibited porosities values around 90% without significant differences with respect to that of the neat scaffold (Table 1). These high porosity values have been found to be suitable to facilitate the process of vascularization and bone tissue reconstruction when polymeric scaffolds are in vivo implanted.^{22,23} On the other hand, elastic modulus of PDLLA scaffold was significantly increased only when 10 wt. % of 2Cu-nBG nanoparticle was incorporated into the polymer matrix (Figure 4). Mechanical reinforcement effect in the polymer nanocomposites depend on the chemical nature, size, content, and distribution of the particles, which determine interfacial interactions and restrictions in the mobility of the polymer chains.²⁴ It has been found that the rigidity of some inorganic fillers may reduce the interfacial energy and consequently enhance the polymer mechanical properties as compared to softer fillers.^{25,26} This effect could explain why 2Cu-nBG nanoparticle having higher metal content produces a more significant mechanical reinforcement in the PDLLA polymer matrix.

The ability of the nanocomposite scaffolds to induce the formation of bone-like apatite on its surface was assessed in SBF at 7 days of incubation. The evolution of apatite formation on the scaffold surfaces was analysed by XRD, ATR-FTIR, and SEM

(Figure 5). Most of the XRD diffractograms of scaffolds immersed in SBF exhibited a peak around 29° associated to the formation of calcite (CaCO_3),²⁷ and some of them exhibit the more characteristic apatite peak at 31.7° , corresponding to the 211 reflections of the apatite crystal (JCPD 205166). ATR-FTIR analysis only detected the formation of apatite on the nanocomposite scaffolds loaded with 10 wt. % of nanoparticles, as judged by the bands at 560 cm^{-1} and 610 cm^{-1} , assigned to the P-O bending vibration in crystalline apatite.²¹ SEM examination of the 10 %wt. nanocomposites confirmed the presence of mineral deposits associated to the formation of apatite on their surface (Figure 5). This effect is consequence of the already demonstrated capacity of nBG to induce rapid crystallization of apatite when incorporated into different biodegradable polymer matrices.^{15,16} Interestingly, copper incorporated into the nBG structure does not alter its in vitro bioactivity, which can be explained by the comparable crystallinity of nBG with those doped with Cu, which would produce a similar dissolution rate of the nanoparticles during the apatite formation process. Cytocompatibility of the scaffolds was assessed using DPSCs until 14 days of incubation. In general, MTS absorbance values of mitochondrial activity of cells cultured with the nanocomposites (Figure 6) tended to be lower than of those incubated with the neat PDLLA scaffold. At 14 days, no significant differences were detected between viability of cells cultured with nBG/PDLLA and most of the Cu-nBG/PDLLA samples. This result suggests that cell viability decrease is related with the incorporation of nanoparticles into the polymer matrix rather than the presence of Cu in the nBG structure. The preparation and bioactive properties of PDLLA scaffolds loaded with nanosized BG has been scantily studied. Hong et al.²⁸ prepared nBG/PDLLA scaffolds with good in vitro bioactivity in SBF, however no cell assays were performed. In the current study, the viability decrease observed in the cells cultured with the nBG nanocomposite scaffolds could be due to the use of quaternary nBG, which has shown lead to higher pH value of the culture medium²⁹ than the ternary nBG.²⁷ Despite the MTS viability decrease detected in cells cultured with the nanocomposites, SEM analysis (Figure 7) revealed the presence of cells intimately adhered on the surface of nanocomposite scaffolds, which is also considered an indicator of the material bioacompatibility. It is for that reason that the nanocomposites were able to stimulate the expression of ALP enzyme (Figure 8), producing some ALP activity values higher than those achieved with the neat PDLLA scaffold. The results also show that the presence of Cu in the scaffold materials does not impair the ALP activity in the DPSCs. ALP is a typical marker of the osteogenic differentiation process of stem cells, which is produced when specialized bone – forming cell lay down the bone extracellular matrix.³⁰ Although some works have reported an increase of ALP activity attributed to copper ions released from the material toward the cell culture medium,^{10,31} most of the studies indicate that Cu does not improve the osteogenic differentiation process.^{11,32–34} So, the capacity of the nCu/PDLLA nanocomposite scaffolds to stimulate the osteogenic cell differentiation should be consequence of the ionic dissolution products of nBG. Specific concentrations of silicon and calcium ions produced by BG recreate an extracellular environment capable of driving the stem cell differentiation toward an osteoblast phenotype.^{35–37} Antibacterial properties of the scaffolds were assessed by measuring the growth of *S. aureus* on the materials (Figure 9). No statistically significant differences were found between the scaffolds with respect to their capacity to inhibit the bacterial growth. It was expected that the nanocomposite scaffolds would exhibit higher antibacterial activity due to the presence of both BG and Cu into their structure. It is well accepted the hypothesis that BG has antibacterial activity due to the increase in local pH following the exchange of sodium ions with protons in body fluids.³⁸ Likewise, microparticles of BG modified with Cu have shown to inhibit the bacterial growth^{8,9} through multiple action mechanisms of Cu ions released from the glass structure. These antimicrobial mechanisms depend on the capacity of the BG particles to dissolve in the physiological medium, which is favoured by the amorphous characteristics of the glass.^{39,40} Figure 10 shows that the concentration of Cu^{2+} released by the 1Cu-nBG (10%)/PDLLA is ~ 0.5 ppm after 14 days, which is six times lower than that reported using micro-BG modified with Cu.¹² The high crystallinity exhibited by the synthesized nBG and Cu-nBG nanoparticles and consequently their reduced solubility could explain the low copper release and the no significant antibacterial activity presented by the nanocomposite scaffolds. In addition, polymeric matrix of the nanocomposite may add diffusion resistance to the ionic dissolution products of the nanoparticle, reducing thus their concentration in the physiological medium. Although the results of this work show that Cu-doped BG nanoparticles can be used to design nanocomposite scaffolds with capacity to stimulate osteogenic markers. The development of antibacterial properties in this type of biomaterials require further studies. The control of sol-gel synthesis parameters to produce Cu – containing glass nanoparticles with amorphous and more soluble structure should be specially addressed. In addition, the optimization of nanoparticle content in the composite, as well as the polymer degradability properties to ensure the adequate exposition of the bioactive components should be also reconsidered.

Conclusions

Synthesis of Cu-containing BG nanoparticles using the $60\text{SiO}_2: 25\text{CaO}:11\text{Na}_2\text{O}: 4\text{P}_2\text{O}_5$ sol-gel system produces particles with relatively crystalline structure. PDLLA nanocomposite scaffolds prepared with Cu-nBG nanoparticles are cytocompatible, promote the formation of bone-like apatite in SBF and stimulate the osteogenic differentiation process of stem cells in vitro. Development of greater antibacterial activity in the nanocomposite scaffolds would requires further research primarily related to the synthesis of Cu-nBG nanoparticles with more amorphous and soluble structure.

Acknowledgements

The authors acknowledge the financial support of U-Redes Consolidación Project URC 026/16 and PRI-ODO 18/004 from University of Chile, and FONDEQUIP EQM130076.

Declaration of conflicting interests

The author(s) declared no potential conflicts of interest with respect to the research, authorship, and/or publication of this article.

Funding

The author(s) disclosed receipt of the following financial support for the research, authorship, and/or publication of this article: This study is supported by University of Chile (Project URC 026/16 and PRI-ODO 18/004) and FONDEQUIP (EQM130076). CONICYT for funding of Basal Centre, CeBiB, FB0001 and P09-022-F from ICM-ECONOMIA, Chile.

ORCID iD

Cristian Covarrubias  <https://orcid.org/0000-0001-8593-7596>

References

1. Winkler T, Sass FA, Duda GN, et al. A review of biomaterials in bone defect healing, remaining shortcomings and future opportunities for bone tissue engineering. *Bone Joint Res* 2018; 7: 232–243.
2. Jin G-Z and Kim H-W. Nanocomposite bioactive polymeric scaffold promotes adhesion, proliferation and osteogenesis of rat bone marrow stromal cells. *Tissue Eng Regen Med* 2014; 11: 284–290.
3. Kaliva M, Chatzinikolaïdou M and Vamvakaki M. *Smart materials for tissue engineering: applications*. London, UK: The Royal Society of Chemistry, 2017, pp. 1–38.
4. Kremers HM, Nwojo ME, Ransom JE, et al. Trends in the epidemiology of osteomyelitis. *J Bone Joint Surg Am* 2015; 97: 837–845.
5. Nazir MA. Prevalence of periodontal disease, its association with systemic diseases and prevention. *Int J Health Sci (Qassim)* 2017; 11: 72–80.
6. Camacho-Flores BA, Martínez-Álvarez O, Arenas-Arrocena MC, et al. Copper: synthesis techniques in nanoscale and powerful application as an antimicrobial agent. *J Nanomater* 2015; 2015: 1–10.
7. Sen CK, Khanna S, Venojarvi M, et al. Copper-induced vascular endothelial growth factor expression and wound healing. *Am J Physiol Circ Physiol* 2002; 282: H1821–H1827.
8. Wu C, Zhou Y, Xu M, et al. Copper-containing mesoporous bioactive glass scaffolds with multifunctional properties of angiogenesis capacity, osteostimulation and antibacterial activity. *Biomaterials* 2013; 34: 422–433.
9. Bari A, Bloise N, Fiorilli S, et al. Copper-containing mesoporous bioactive glass nanoparticles as multifunctional agent for bone regeneration. *Acta Biomater* 2017; 55: 493–504.
10. Zheng K, Dai X, Lu M, et al. Synthesis of copper-containing bioactive glass nanoparticles using a modified Stöber method for biomedical applications. *Colloids Surf B Biointerfaces* 2017; 150: 159–167.
11. Bejarano J, Caviedes P and Palza H. Sol–gel synthesis and in vitro bioactivity of copper and zinc-doped silicate bioactive glasses and glass-ceramics. *Biomed Mater* 2015; 10: 025001.
12. Bejarano J, Detsch R, Boccaccini AR, et al. PDLLA scaffolds with Cu- and Zn-doped bioactive glasses having multifunctional properties for bone regeneration. *J Biomed Mater Res A* 2017; 105: 746–756.
13. Jones JR. New trends in bioactive scaffolds: the importance of nanostructure. *J Eur Ceram Soc* 2009; 29: 1275–1281.
14. Covarrubias C, Arroyo F, Balanda C, et al. The effect of the nanoscale structure of nanobioceramics on their in vitro bioactivity and cell differentiation properties. *J Nanomater* 2015; 2015: 1–14.
15. Covarrubias C, Cádiz M, Maureira M, et al. Bionanocomposite scaffolds based on chitosan–gelatin and nanodimensional bioactive glass particles: in vitro properties and in vivo bone regeneration. *J Biomater Appl* 2018; 32: 1155–1163.
16. Covarrubias C, Agüero A, Maureira M, et al. In situ preparation and osteogenic properties of bionanocomposite scaffolds based on aliphatic polyurethane and bioactive glass nanoparticles. *Mater Sci Eng C* 2019; 96: 642–653.
17. Kokubo T, Kushitani H, Sakka S, et al. Solutions able to reproduce in vivo surface-structure changes in bioactive glass-ceramic A-W3. *J Biomed Mater Res* 1990; 24: 721–734.
18. Covarrubias C, Trepiana D and Corral C. Synthesis of hybrid copper-chitosan nanoparticles with antibacterial activity against cariogenic *Streptococcus mutans*. *Dent Mater J* 2018; 37: 379–384.
19. Lin C-C, Huang L-C and Shen P. Na₂CaSi₂O₆–P₂O₅ based bioactive glasses. Part 1: elasticity and structure. *J Non Cryst Solids* 2005; 351: 3195–3203.
20. Lefebvre L, Chevalier J, Gremillard L, et al. Structural transformations of bioactive glass 45S5 with thermal treatments. *Acta Mater* 2007; 55: 3305–3313.
21. Hench LL and Wilson J. *An introduction to bioceramics*. 2nd ed. London, UK: Imperial College Press, 2013, pp. 530–531.
22. Karageorgiou V and Kaplan D. Porosity of 3D biomaterial scaffolds and osteogenesis. *Biomaterials* 2005; 26: 5474–5491.
23. Cheng MQ, Wahafu T, Jiang GF, et al. A novel open-porous magnesium scaffold with controllable microstructures and properties for bone regeneration. *Sci Rep* 2016; 6: 24134.
24. Padmanabhan KA. Mechanical properties of nanostructured materials. *Mater Sci Eng A* 2001; 304–306: 200–205.
25. Kiran MD, Govindaraju HK, Jayaraju T, et al. Review-Effect of fillers on mechanical properties of polymer matrix composites. *Mater Today Proc* 2018; 5: 22421–22424.
26. Liang C, Song P, Gu H, et al. Nanopolydopamine coupled fluorescent nanozinc oxide reinforced epoxy nanocomposites. *Compos A Appl Sci Manuf* 2017; 102: 126–136.

27. Valenzuela F, Covarrubias C, Martínez C, et al. Preparation and bioactive properties of novel bone-repair bionanocomposites based on hydroxyapatite and bioactive glass nanoparticles. *J Biomed Mater Res B Appl Biomater* 2012; 100B: 1672–1682.
28. Hong Z, Reis RL and Mano JF. Preparation and in vitro characterization of scaffolds of poly(l-lactic acid) containing bioactive glass ceramic nanoparticles. *Acta Biomater* 2008; 4: 1297–1306.
29. Ben-Arfa BAE, Fernandes HR, Miranda Salvado IM, et al. Synthesis and bioactivity assessment of high silica content quaternary glasses with Ca: P ratios of 1.5 and 1.67, made by a rapid sol-gel process. *J Biomed Mater Res A* 2018; 106: 510–520.
30. Blair HC, Larrouture QC, Li Y, et al. Osteoblast differentiation and bone matrix formation in vivo and in vitro. *Tissue Eng B Rev* 2017; 23: 268–280.
31. Burghardt I, Lüthen F, Prinz C, et al. A dual function of copper in designing regenerative implants. *Biomaterials* 2015; 44: 36–44.
32. Rodríguez JP, Ríos S and González M. Modulation of the proliferation and differentiation of human mesenchymal stem cells by copper. *J Cel Biochem* 2002; 85: 92–100.
33. Lai YL and Yamaguchi M. Effects of copper on bone component in the femoral tissues of rats: anabolic effect of zinc is weakened by copper. *Biol Pharm Bull* 2005; 28: 2296–2301.
34. Rath SN, Brandl A, Hiller D, et al. Bioactive copper-doped glass scaffolds can stimulate endothelial cells in co-culture in combination with mesenchymal stem cells. *PLoS One* 2014; 9: e113319.
35. Xynos ID, Edgar AJ, Buttery LDK, et al. Gene-expression profiling of human osteoblasts following treatment with the ionic products of bioglass 45S5 dissolution. *J Biomed Mater Res* 2001; 55: 151–157.
36. Tsigkou O, Jones JR, Polak JM, et al. Differentiation of fetal osteoblasts and formation of mineralized bone nodules by 45S5 Bioglass® conditioned medium in the absence of osteogenic supplements. *Biomaterials* 2009; 30: 3542–3550.
37. Kaur G, Sriranganathan N, Waldrop SG, et al. Effect of copper on the up-regulation/down-regulation of genes, cytotoxicity, and ion dissolution for mesoporous bioactive glasses. *Biomed Mater* 2017; 12: 045020.
38. Drago L, Toscano M, Bottagisio M, et al. Recent evidence on bioactive glass antimicrobial and antibiofilm activity: a mini-review. *Materials (Basel)* 2018; 11: 326.
39. Filho OP, La Torre GP and Hench LL. Effect of crystallization on apatite-layer formation of bioactive glass 45S5. *J Biomed Mater Res* 1996; 30: 509–514.
40. Magallanes-Perdomo M, Meille S, Chenal J-M, et al. Bioactivity modulation of Bioglass® powder by thermal treatment. *J Eur Ceram Soc* 2012; 32: 2765–2775.